REVIEW

doi:10.1038/nature12908

Solar System evolution from compositional mapping of the asteroid belt

F. E. DeMeo[1,2] & B. Carry[3,4]

Advances in the discovery and characterization of asteroids over the past decade have revealed an unanticipated underlying structure that points to a dramatic early history of the inner Solar System. The asteroids in the main asteroid belt have been discovered to be more compositionally diverse with size and distance from the Sun than had previously been known. This implies substantial mixing through processes such as planetary migration and the subsequent dynamical processes.

Although studies of exoplanetary systems have the advantage of numbers[1] to answer the question of how planetary systems are built, our Solar System has the advantage of detail. For nearly two centuries since their first discovery, asteroids have been viewed as remnants of planetary formation. Located between Mars and Jupiter in the main asteroid belt (Fig. 1), they were thought to have formed essentially where they now are[2].

Early measurements showed asteroids in the inner part of the main asteroid belt were more reflective and appear subtly 'redder' than the outer, 'bluer' ones[3–6]. In the 1980s, distinct colour groupings of major asteroid compositional types were discovered as a function of distance from the Sun[2]. In the classic theory, this was interpreted as the remnant of a thermal gradient across the main belt at the time the Solar System formed[2,7–9]. An understanding of that gradient promised to hold clues to the initial conditions during planet formation.

Yet, over the course of the discovery of over half a million asteroids since the 1980s, the idea of a static Solar System history has dramatically shifted to one of great dynamic change and mixing. Driving this view was the effect on the main asteroid belt of planetary migration models that aimed to recreate the structure of the rest of the Solar System, such as the orbits of the giant planets, Pluto and the transneptunian objects, and the Jupiter Trojan asteroids (which reside in the L4 and L5 Lagrange points of Jupiter's orbit)[10–13].

As the planetary migration models evolved, so also new compositional characteristics of the main belt were uncovered through observation that were increasingly inconsistent with the classic theory. At first, just a few rogue asteroids were found to be contaminating the distinct groupings[14–16]. Now, with tens of thousands of asteroids to analyse for which we have compositional measurements[17,18], we can see that this mixing of asteroid types is more of the rule, rather than the exception, across the main belt[19].

Today, all the newly revealed aspects of the main asteroid belt, including its orbital and compositional structure and the dynamical processes that sculpt it, contribute to a more coherent story. In modern dynamical models, the giant planets are thought to have migrated over substantial distances, shaking up the asteroids—which formed throughout the Solar System—like flakes in a snow globe, and transporting some of them to their current locations in the asteroid belt (Fig. 2). The main asteroid belt thus samples the conditions across the entire Solar System. Yet, at the same time, the Hilda asteroids (located 4 AU from the Sun between the main belt and Jupiter (one astronomical unit is approximately the Earth–Sun distance); see Fig. 1) and the Jupiter Trojans appear distinctly homogeneous, challenging us to untangle the various events of the Solar System's evolution. Our Solar System's path to creating the arrangement of the planets today and the conditions that made life on Earth possible will set the context for understanding the myriad of exoplanetary systems.

Send in the rogues

Their generally redder-to-bluer colour and compositional trend implied that asteroids tend to preserve their initial formation environment: the temperature and compositional gradient in that part of the disk at the time of planetesimal formation[2,9]. From what astronomers understood at the time (the 1980s), guided by comparison with meteorites, the reddish (with a positive slope from ultraviolet-to-visible wavelengths) ones filling the inner main belt were melted igneous bodies[20], and the bluish (with a neutral slope from the ultraviolet-to-visible) ones in the outer main belt had undergone little thermal alteration[6]. The goal of the next decade (the 1990s) was to explain how the thermal gradient could be so steep, creating such wildly different outcomes, from melted to primitive over a distance of just 1 AU (ref. 21).

That original interpretation of the compositions of reddish and bluish asteroids was wrong. In fact, direct sampling (by spacecraft[22]) of the reddish asteroid (25143) Itokawa definitively showed that it did experience some heating but was relatively primitive, compared with the previous interpretation of a melted body[23–27]. Although it was still a challenge to explain the asteroids' compositional and thermal trend from warm to cold, it was not as drastic a gradient as had been supposed.

Such compositional measurements for the largest asteroids seemed to explain the gradient better, but the few measurements becoming available for smaller objects were beginning to reveal the misfits. First was (1459) Magnya, a basaltic fragment discovered among the cold, bluish bodies[14]. Then, a handful more of these rogue igneous asteroids were found dispersed across the main asteroid belt[16,28,29]. Iron asteroids present in the main belt should have formed much closer to the Sun[15]. Primitive asteroids were discovered in the inner belt[30], and furthermore, the reddish objects occurred throughout the outer belt[31–33]. Other asteroids that appeared to be dry asteroids were discovered to contain volatiles on or just below the surface, suggesting that they formed beyond the snowline (the distance from the Sun at which the temperature is low enough for water to be ice)[34–38]. At first, these observations seemed to represent 'contamination' by individual, unusual asteroids, but gradually it has become clear that even the core groups of reddish and bluish asteroids were more broadly distributed, further challenging the classic theory of a static Solar System.

[1]Harvard-Smithsonian Center for Astrophysics, 60 Garden Street, MS-16, Cambridge, Massachusetts 02138, USA. [2]Department of Earth, Atmospheric and Planetary Sciences, Massachusetts Institute of Technology (MIT), 77 Massachusetts Avenue, Cambridge, Massachusetts 02139, USA. [3]Institut de Mécanique Céleste et de Calcul des Éphémérides, Observatoire de Paris, UMR8028 CNRS, 77 avenue Denfert-Rochereau, 75014 Paris, France. [4]European Space Astronomy (ESA) Centre, PO Box 78, Villanueva de la Cañada 28691, Madrid, Spain.

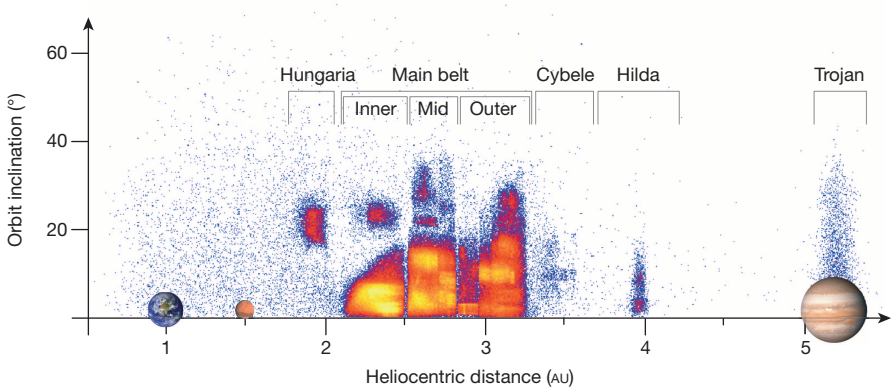

Figure 1 | The asteroid belt in context with the planets. This plot shows the location of the main belt with respect to the planets and the Sun as well as the orbital structure of asteroid inclinations and number density of objects (yellow represents the highest number density, blue the lowest). Asteroids have much higher orbital eccentricities and inclinations than do the planets. The structure of the main belt is divided by unstable regions, seen most prominently at 2.5 AU and 2.8 AU (locations where an asteroid's orbit is 'in resonance' with Jupiter's orbit), that separate the inner, middle and outer sections of the main belt. The Hungaria asteroids are located closer to the Sun than is the main belt and have orbital inclinations centred near 20 degrees. The Hildas are located near 4 AU and the Jupiter Trojans are in the L4 and L5 Lagrange points of Jupiter's orbit.

The compositional medley of asteroids

Equipped with an abundance of visible-wavelength colours and surface-brightness measurements from recent surveys[17,18] we can now reveal a new map of the distribution of asteroids down to diameters of 5 km (ref. 19) (Fig. 3). Traditionally, the distribution has been presented as the relative fraction of asteroid classes as a function of distance[2,9,31,32]. Now we compare bodies ranging from 5 km to 1,000 km in diameter, so an equal weighting would distort the view. By transforming the map of the asteroid belt to the distribution of mass[19,39], we are able to account for each asteroid type accurately, rather than the frequency or number of types (Fig. 3). Furthermore, we can now explore the change in distribution as a function of size (Fig. 4).

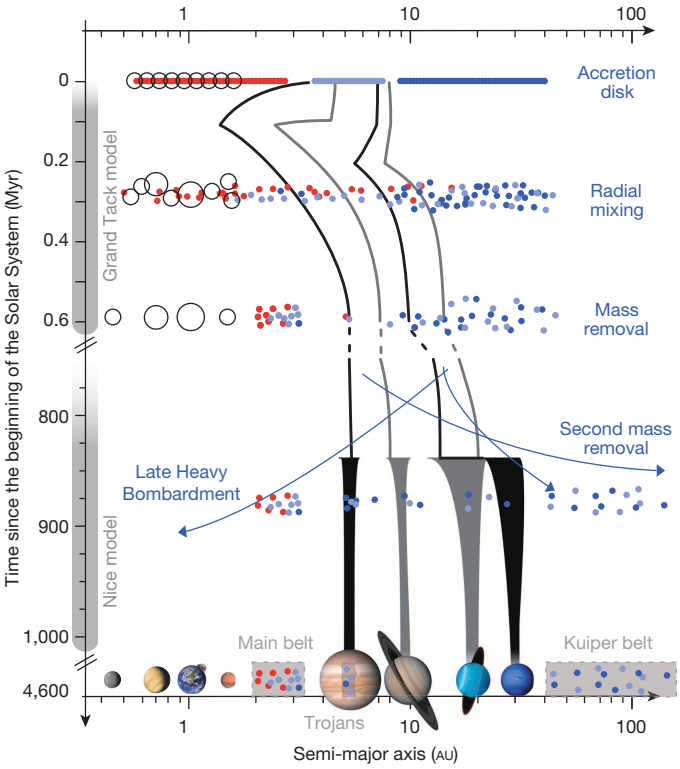

Figure 2 | Cartoon of the effects of planetary migration on the asteroid belt. This figure captures some major components of the dynamical history of small bodies in the Solar System based on models[11,12,51,54]. These models may not represent the actual history of the Solar System, but are possible histories. They contain periods of radial mixing, mass removal and planet migration—ultimately arriving at the current distribution of planets and small-body populations.

This is what we have found. The rarer asteroid types, such as the crust and mantle remnants of fully heated and melted bodies, are seen in all regions of the main belt[14,16]. We do not yet know whether this means that the locations of their respective parent bodies were ubiquitous in the inner Solar System or whether they were created close to the Sun and later injected into the main belt[15,40].

Asteroids that look compositionally Trojan-like (D-types; see Fig. 3) are detected in the inner belt, where they are not predicted to exist by dynamical models[19,41,42]. Their presence so close to the Sun demands an explanation for how they arrived there and whether they are really linked to the Trojan asteroids at all.

The Hungaria region is typically associated with its eponymous and brightest member, (434) Hungaria, and similarly super-reflective asteroids[2,8] (E-types; see Fig. 3). Despite this, most of the mass of this region is contained within a few reddish and bluish objects, which are also common elsewhere in the main belt[43–45].

The relative mass contribution of each asteroid class changes as a function of size in each region of the main belt. Most dramatic is the increase of bluish objects (C-types; see Fig. 3) as size decreases in the inner belt. Although these bluish objects are notoriously rare in the inner belt at large sizes[2,32], where they comprise only 6% of the total mass, half of the mass is bluish at the smallest sizes.

In the outer belt, reddish asteroids (S-types; see Fig. 3) make up a small fraction of the total there, yet their actual mass is still quite significant. In fact, we now find more than half of the mass of reddish objects outside the inner belt[19].

Just over a decade ago, astronomers still clung to the concept of an orderly compositional gradient across the main asteroid belt[46]. Since then the trickle of asteroids discovered in unexpected locations has turned into a river. We now see that all asteroid types exist in every region of the main belt (see Box 1 for a discussion of Hildas and Trojans). The smorgasbord of compositional types of small bodies throughout the main belt contrasts with the compositional groupings at large sizes. All these features demanded major changes in the interpretation of the history of the current asteroid belt and, in turn, of the Solar System.

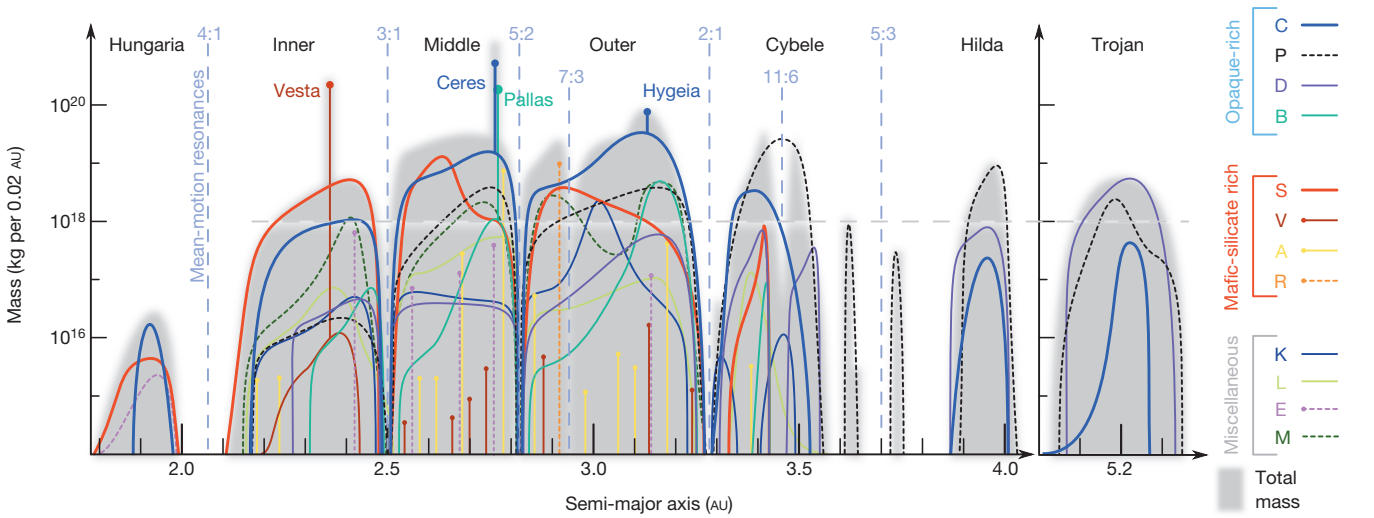

Figure 3 | The compositional mass distribution throughout the asteroid belt out to the Trojans. The grey background is the total mass within each 0.02-AU bin. Each colour represents a unique spectral class of asteroid, denoted by a letter in the key. The horizontal line at 10^{18} kg is the limit of the work from the 1980s[2,8,9]. The upper portion of the plot remains consistent with that work, but immense detail is now revealed at the lower mass range[19].

Cracking the 'compositional code' of the map

Earlier planetesimal-formation theories that explained the history of the asteroid belt invoked turbulence in the nebula, radial decay of material due to gas drag, sweeping resonances and scattered embryos[47,48]. Individually, each mechanism was, however, insufficient, and even together, although many of these mechanisms could deplete, excite and partially mix the main belt, they could not adequately reproduce the current asteroid belt[49].

The concept of planetary migration—whereby the planets change orbits over time owing to gravitational effects from the surrounding dust, gas or planetesimals—was not new, but its introduction as a major driver of the history of the asteroid belt came only recently. Migration models began by explaining the orbital structure and mass distribution of the outer Solar System, including the Kuiper belt past Neptune[50]. Individual models could successfully recreate specific parts, but we still sought to define a consistent set of events that would explain all aspects of the outer Solar System. Every action of the planets causes a reaction in the asteroid belt, so these models also needed to be consistent with the compositional framework within the main belt that we see today.

The Nice model was the first comprehensive solution that could simultaneously explain many unique structural properties of the Solar System[11–13,51,52],

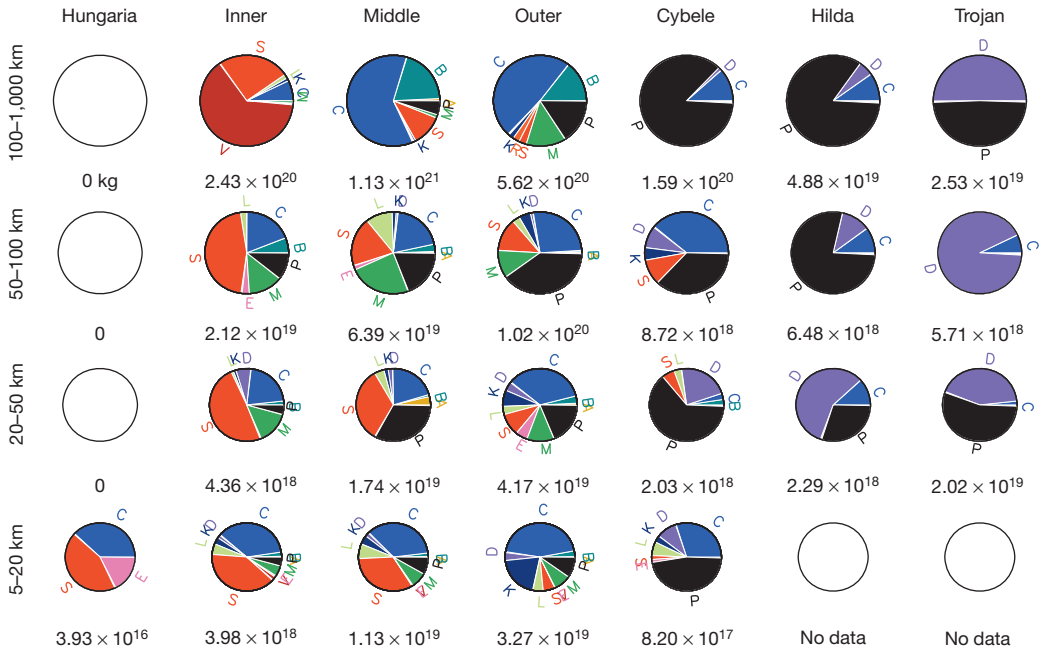

Figure 4 | The compositional mass distribution as a function of size throughout the main belt out to the Trojans. The mass is calculated for each individual object with a diameter of 50 km and greater, using its albedo to determine size and the average density[39] for that asteroid's taxonomic class. For the smaller sizes we determine the fractional contribution of each class at each size and semi-major axis, and then apply that fraction to the distribution of all known asteroids from the Minor Planet Center (http://minorplanetcenter.org/) including a correction for discovery incompleteness at the smallest sizes in the middle and outer belt[19]. Asteroid mass is grouped according to objects within four size ranges, with diameters of 100–1,000 km, 50–100 km, 20–50 km and 5–20 km. Seven zones are defined as in Fig. 1: Hungaria, inner belt, middle belt, outer belt, Cybele, Hilda and Trojan. The total mass of each zone at each size is labelled and the pie charts mark the fractional mass contribution of each unique spectral class of asteroid. The total mass of Hildas and Trojans are underestimated because of discovery incompleteness. The relative contribution of each class changes with both size and distance.

BOX 1

The Hilda and Trojan asteroids

The Hilda and Jupiter Trojan asteroids are located beyond the main asteroid belt at 4 AU and 5.2 AU, respectively (Fig. 1). The asteroid types in these regions are physically distinct from the main belt and from each other: the largest Hildas are dominated by spectral P-type asteroids and the largest Trojans are dominated by D-types[2] (Fig. 3). Despite interlopers of all types becoming more common throughout the main belt, the Hildas and Trojans remained curiously distinct and homogeneous.

Continued observations find that bright objects among Hildas and Trojans are scarce even at the small size scales[78–85]. It was recently and unexpectedly discovered, however, that the smallest bodies in these regions break rank (Fig. 4): most of the small Hildas have physical properties more similar to Trojans (D-type) and the makeup of the Trojans also changes with size with differing fractions of D-types and Hilda-like P-types[19,86,87]. Migration scenarios can now explain why the Hildas and Trojans look so different from the main belt, but they cannot yet explain the important details of why they look distinct from each other at the largest sizes (in relative fraction of the D-type and P-type asteroids) and are also different at the smaller sizes.

such as the locations of the giant planets and their orbital eccentricities[11], capture of the irregular satellites of Saturn[53], and the orbital properties of the Trojans[12] (Fig. 2). In the original model, Jupiter moves inward while the other giant planets migrate outward. As Jupiter and Saturn cross their 1:2 mean motion resonance, the system is destabilized[11]. In the most recent version of this model, the interaction between the giant planets and a massive, distant Kuiper disk causes the system to destabilize[13]. At that point, the primordial Jupiter Trojan region is emptied. Bodies that were scattered inward from beyond Neptune then repopulate this region. By reproducing the Trojans' orbital distributions and mass, the Nice model also naturally explains the why the Trojan region is compositionally distinct from the main belt: it would be populated solely by outer Solar System bodies and would not contain locally formed asteroids.

Missing from the Nice model, however, was an explanation of the large-scale mixing of reddish and bluish material in the asteroid belt that was becoming increasingly prominent. The Grand Tack model[54] showed that during the time of terrestrial planet formation (before the events of the Nice model would have taken place), Jupiter could have migrated as close to the Sun as Mars is today. Jupiter would have moved right through the primordial asteroid belt, emptying it and then repopulating it with scrambled material from both the inner and outer Solar System as Jupiter then reversed course and headed back towards the outer Solar System. Once the details of the resulting distribution in the Grand Tack model have been closely compared to the emerging observational picture, it will become clear whether this model can crack the asteroid belt's 'compositional code'.

Planetary migration ends well within the first billion years of our Solar System's 4.5-billion-year history. The asteroid belt, however, is still dynamic today. Collisions between asteroids are continuously grinding the bodies down to smaller and smaller sizes. The smaller ones ($<$40 km) are then subject to the Yarkovsky effect, according to which uneven diurnal heating and cooling of the body alters its orbit[55–59]. The Yarkovsky effect thoroughly mixes small bodies within each section of the main belt, but once they reach a major resonance—such as the 3:1 and 5:2 mean motion resonances at the locations where the orbital periods of an asteroid and of Jupiter are related by integers—they are swiftly ejected from the main belt[57–59]. Current observations[60,61] and models[28,62–64] indicate that the strong resonances with Jupiter inhibit the crossing of material from one region to another. These processes continue to mould the asteroid belt, erasing some of its past history and creating new structures in this complex system.

New observational evidence that reveals a greater mixing of bodies supports the idea of a Solar System that was and continues to be in a state of evolution and flux. Indeed, dynamical models have been leading us step-by-step to interpret the asteroid belt as a melting pot of bodies arriving from diverse backgrounds. Dynamical models have come a long way, but they have yet to explain the dichotomy between the orderly trend among the largest asteroids and the increased mixing of asteroid types at smaller sizes. Particularly noticeable are the scatter of igneous bodies and the existence of asteroids that look physically similar to Trojans in the inner belt. These details promise to teach us how our Solar System was built, providing context for other planetary systems.

The future

The ultimate goal of asteroid studies is to complete the picture of where these bodies formed and how they relate to the current chemistry and volatile abundance on Earth. No longer is our Solar System just an isolated example, and with only a minimal speculative extrapolation, asteroid-like building blocks seem likely to have influenced countless terrestrial-like planetary systems. The ongoing hunt for Earth-like planets has as its corollary the hunt for possible signatures of asteroid-like zones and an assessment of their uniqueness or commonality in all planetary systems.

Even though we now know the asteroid distributions in the Solar System down to 5 km, we are still literally only scratching the surface of what can be known about them. Asteroid interiors are the *terra incognita* for the next generation of asteroid researchers. At present we are frustrated by the inability of most physical measurements to provide any information on the interior of an asteroid. An asteroid's interior reveals its thermal history, which constrains the initial conditions of the protoplanetary disk during planetesimal formation. NASA's Dawn spacecraft mission recently provided a glimpse inside Vesta, determining the core mass fraction of this large asteroid from shape and gravity measurements[65]. When Dawn visits Ceres, we will learn to what extent this large asteroid differentiated into an ice mantle and rocky core[66–68]. Increased measurements of asteroid densities, provided mainly by the study of binary asteroids, will help us to infer their interior structure[39].

Each of our broad asteroid classes probably encompasses a wide variety of surface compositions[69,70]. Our meteorite collection has provided significant detail about the range of asteroid compositions, but to make firm links between the asteroids and meteorites, we need to observe an asteroid in space and then measure the same body in a laboratory. This will be achieved by asteroid sample return missions that are already under way[71–73], as well as 'free sample return' by meteorite falls such as the serendipitously discovered Almahata Sitta meteorite (formerly asteroid 2008 TC_3)[74,75].

Finally, the next step in distribution trends is to complement a refined understanding of asteroid compositions with physical measurements capable of detecting that detail on a large scale. The compositional trends discussed up to now cover broad taxonomic classes and combine objects into just a few major groups that do not accurately reflect the complexity of the asteroids' original and current compositions. Higher-spectral-resolution large-scale surveys at visible[76,77] and near- to mid-infrared wavelengths combined with the already available albedo information for hundreds of thousands of asteroids would be the most realistic data set to attain over the next decade or two.

Received 10 July; accepted 22 November 2013.

1. Wright, J. T. *et al.* The Exoplanet Orbit Database. *Publ. Astron. Soc. Pacif.* **123,** 412–422 (2011).
2. Gradie, J. & Tedesco, E. Compositional structure of the asteroid belt. *Science* **216,** 1405–1407 (1982).
This is a comprehensive view of the compositional trends of the asteroid belt that served for decades as the backbone for interpretations of the main belt.
3. Fischer, H. Farbmessungen an kleinen planeten. *Astron. Nachr.* **272,** 127–147 (1941).
4. Wood, X. H. J. & Kuiper, G. P. Photometric studies of asteroids. *Astrophys. J.* **137,** 1279–1285 (1963).
5. Chapman, C. R., Johnson, T. V. & McCord, T. B. in *Proc. IAU Colloq. 12* (ed. Gehrels, T.) SP 267, 1–47 (National Aeronautics and Space Administration, 1971).
6. Chapman, C. R., Morrison, D. & Zellner, B. Surface properties of asteroids—a synthesis of polarimetry, radiometry, and spectrophotometry. *Icarus* **25,** 104–130 (1975).

7. Zellner, B., Tholen, D. J. & Tedesco, E. F. The eight-color asteroid survey—results for 589 minor planets. *Icarus* **61,** 355–416 (1985).
8. Gradie, J. C., Chapman, C. R. & Tedesco, E. F. in *Asteroids II* (eds Binzel, R. P., Gehrels, T. & Matthews, M. S.) 316–335 (Univ. Arizona Press, 1989).
9. Bell, J. F., Davis, D. R., Hartmann, W. K. & Gaffey, M. J. in *Asteroids II* (eds Binzel, R. P., Gehrels, T. & Matthews, M. S.) 921–945 (Univ. Arizona Press, 1989).
10. Malhotra, R. The origin of Pluto's peculiar orbit. *Nature* **365,** 819–821 (1993).
11. Tsiganis, K., Gomes, R., Morbidelli, A. & Levison, H. F. Origin of the orbital architecture of the giant planets of the Solar System. *Nature* **435,** 459–461 (2005).
12. Morbidelli, A., Levison, H. F., Tsiganis, K. & Gomes, R. Chaotic capture of Jupiter's Trojan asteroids in the early Solar System. *Nature* **435,** 462–465 (2005).
13. Levison, H. F., Morbidelli, A., Tsiganis, K., Nesvorny, D. & Gomes, R. Late orbital instabilities in the outer planets induced by interaction with self-gravitating planetesimal disk. *Astron. J.* **142,** 152 (2011).
14. Lazzaro, D. *et al.* Discovery of a basaltic asteroid in the outer main belt. *Science* **288,** 2033–2035 (2000).
15. Bottke, W. F., Nesvorny, D., Grimm, R. E., Morbidelli, A. & O'Brien, D. P. Iron meteorites as remnants of planetesimals formed in the terrestrial planet region. *Nature* **439,** 821–824 (2006).
16. Moskovitz, N. A. *et al.* The distribution of basaltic asteroids in the main belt. *Icarus* **198,** 77–90 (2008).
17. Ivezić, Z. *et al.* Solar System objects observed in the Sloan Digital Sky Survey commissioning data. *Astron. J.* **122,** 2749–2784 (2001).
This is the original article on asteroid measurements from the Sloan Digital Sky Survey (SDSS), which provided multi-filter photometry in the visible spectrum for over 100,000 asteroids.
18. Mainzer, A. *et al.* Preliminary Results from NEOWISE: an enhancement to the Wide-field Infrared Survey Explorer for Solar System science. *Astrophys. J.* **731,** 53 (2011).
This is the original article on asteroid measurements from the Wide-field Infrared Survey Explorer (WISE), which provides diameters and albedos (surface brightness) for over 100,000 asteroids.
19. DeMeo, F. E. & Carry, B. The taxonomic distribution of asteroids from multi-filter all-sky photometric surveys. *Icarus* **226,** 723–741 (2013).
This work created a new framework to quantify the compositional makeup of the asteroid belt by looking at the distribution by mass rather than numbers.
20. McCord, T. B. & Gaffey, M. J. Asteroids—surface composition from reflection spectroscopy. *Science* **186,** 352–355 (1974).
21. Grimm, R. E. & McSween, H. Y. Heliocentric zoning of the asteroid belt by aluminum-26 heating. *Science* **259,** 653–655 (1993).
22. Nakamura, T. *et al.* Itokawa dust particles: a direct link between S-type asteroids and ordinary chondrites. *Science* **333,** 1113–1116 (2011).
23. Chapman, C. R. S-type asteroids, ordinary chondrites, and space weathering: the evidence from Galileo's fly-bys of Gaspra and Ida. *Meteorit. Planet. Sci.* **31,** 699–725 (1996).
24. Sasaki, S. *et al.* Production of iron nanoparticles by laser irradiation in a simulation of lunar-like space weathering. *Nature* **410,** 555–557 (2001).
25. Chapman, C. R. Space weathering of asteroid surfaces. *Annu. Rev. Earth Planet. Sci.* **32,** 539–567 (2004).
26. Brunetto, R. *et al.* Space weathering of silicates simulated by nanosecond pulse UV excimer laser. *Icarus* **180,** 546–554 (2006).
27. Binzel, R. P., Rivkin, A. S., Bus, S. J., Sunshine, J. M. & Burbine, T. H. MUSES-C target asteroid (25143) 1998 SF36: a reddened ordinary chondrite. *Meteorit. Planet. Sci.* **36,** 1167–1172 (2001).
28. Roig, F., Ribeiro, A. O. & Gil-Hutton, R. Taxonomy of asteroid families among the Jupiter Trojans: comparison between spectroscopic data and the Sloan Digital Sky Survey colors. *Astron. Astrophys.* **483,** 911–931 (2008).
29. Carvano, J. M., Hasselmann, H., Lazzaro, D. & Mothé-Diniz, T. SDSS-based taxonomic classification and orbital distribution of main belt asteroids. *Astron. Astrophys.* **510,** A43 (2010).
30. Clark, B. E., Bell, J. F., Fanale, F. P. & O'Connor, D. J. Results of the seven-color asteroid survey: infrared spectral observations of ~50-km size S-, K-, and M-type asteroids. *Icarus* **113,** 387–402 (1995).
31. Bus, S. J. & Binzel, R. P. Phase II of the Small Main-Belt Asteroid Spectroscopic Survey: a feature-based taxonomy. *Icarus* **158,** 146–177 (2002).
32. Mothé-Diniz, T., Carvano, J. & Lazzaro, D. Distribution of taxonomic classes in the main belt of asteroids. *Icarus* **162,** 10–21 (2003).
This was the first extensive look at asteroid compositional distributions at smaller sizes; it indicates that the distribution differs from that in ref. 2.
33. Lazzaro, D. *et al.* S3OS2: the visible spectroscopic survey of 820 asteroids. *Icarus* **172,** 179–220 (2004).
34. Hsieh, H. & Jewitt, D. A population of comets in the main asteroid belt. *Science* **312,** 561–563 (2006).
35. Campins, H. *et al.* Water ice and organics on the surface of the asteroid 24 Themis. *Nature* **464,** 1320–1321 (2010).
36. Rivkin, A. S. & Emery, J. P. Detection of ice and organics on an asteroidal surface. *Nature* **464,** 1322–1323 (2010).
37. Licandro, J. *et al.* (65) Cybele: detection of small silicate grains, water-ice, and organics. *Astron. Astrophys.* **525,** A34 (2011).
38. Jewitt, D. The active asteroids. *Astron. J.* **143,** 66 (2012).
39. Carry, B. Density of asteroids. *Planet. Space Sci.* **73,** 98–118 (2012).
This work conducted a detailed analysis of 994 mass estimates and 1,500 volume determinations of 300 asteroids, demonstrating density trends per asteroid taxonomic class.
40. Elkins-Tanton, L. T., Weiss, B. P. & Zuber, M. T. Chondrites as samples of differentiated planetesimals. *Earth Planet. Sci. Lett.* **305,** 1–10 (2011).
41. DeMeo, F. E., Binzel, R. P., Carry, B., Polishook, D. & Moskovitz, N. A. Unexpected D-type interlopers in the inner main belt. *Icarus* **229,** 392–399 (2014).
42. Levison, H. *et al.* Contamination of the asteroid belt by primordial trans-Neptunian objects. *Nature* **460,** 364–366 (2009).
43. Carvano, J. M., Lazzaro, D., Mothé-Diniz, T., Angeli, C. A. & Florczak, M. Spectroscopic survey of the Hungaria and Phocaea dynamical groups. *Icarus* **149,** 173–189 (2001).
44. Assandri, M. C. & Gil-Hutton, R. Surface composition of Hungaria asteroids from the analysis of the Sloan Digital Sky Survey colors. *Astron. Astrophys.* **488,** 339–343 (2008).
45. Warner, B., Harris, A. W., Vokrouhlicky, D., Nesvorny, D. & Bottke, W. F. Analysis of the Hungaria asteroid population. *Icarus* **204,** 172–182 (2009).
46. Meibom, A. & Clark, B. E. Evidence for the insignificance of ordinary chondritic material in the asteroid belt. *Meteorit. Planet. Sci.* **34,** 7–24 (1999).
47. Ruzmaikina, T. V., Safronov, V. S. & Weidenschilling, S. J. in *Asteroids II* (eds Binzel, R. P., Gehrels, T. & Matthews, M. S.) 681–700 (Univ. Arizona Press, 1989).
48. Petit, J. M., Chambers, J., Franklin, F. & Nagasawa, M. in *Asteroids III* (eds Bottke, W. F., Cellino, A., Paolicchi, P. & Binzel, R. P.) 711–723 (Univ. Arizona Press, 2002).
49. O'Brien, D. P., Morbidelli, A. & Bottke, W. F. The primordial excitation and clearing of the asteroid belt—revisited. *Icarus* **191,** 434–452 (2007).
50. Gomes, R. The origin of the Kuiper Belt high-inclination population. *Icarus* **161,** 404–418 (2003).
51. Gomes, R., Levison, H. F., Tsiganis, K. & Morbidelli, A. Origin of the cataclysmic Late Heavy Bombardment period of the terrestrial planets. *Nature* **435,** 466–469 (2005).
52. Morbidelli, A., Tsiganis, K., Crida, A., Levison, H. F. & Gomes, R. Dynamics of the giant planets of the solar system in the gaseous protoplanetary disk and their relationship to the current orbital architecture. *Astron. J.* **134,** 1790–1798 (2007).
53. Nesvorny, D., Vokrouhlický, D. & Morbidelli, A. Capture of irregular satellites during planetary encounters. *Astron. J.* **133,** 1962 (2007).
54. Walsh, K. J., Morbidelli, A., Raymond, S. N., O'Brien, D. P. & Mandell, A. M. A low mass for Mars from Jupiter's early gas-driven migration. *Nature* **475,** 206–209 (2011).
55. Chesley, S. R. *et al.* Direct detection of the Yarkovsky effect by radar ranging to asteroid 6489 Golevka. *Science* **302,** 1739–1742 (2003).
56. Bottke, W. F., Vokrouhlický, D., Rubincam, D. P. & Nesvorný, D. The Yarkovsky and YORP effects: implications for asteroid dynamics. *Annu. Rev. Earth Planet. Sci.* **34,** 157–191 (2006).
57. Gladman, B. J. *et al.* Dynamical lifetimes of objects injected into asteroid belt resonances. *Science* **277,** 197–201 (1997).
58. Farinella, P., Vokrouhlicky, D. & Hartmann, W. K. Meteorite delivery via Yarkovsky orbital drift. *Icarus* **132,** 378–387 (1998).
59. Bottke, W. F., Vokrouhlicky, D., Broz, M., Nesvorny, D. & Morbidelli, A. Dynamical spreading of asteroid families by the Yarkovsky effect. *Science* **294,** 1693–1696 (2001).
60. Parker, A. *et al.* The size distributions of asteroid families in the SDSS Moving Object Catalog 4. *Icarus* **198,** 138–155 (2008).
61. Masiero, J. R. *et al.* Asteroid family identification using the hierarchical clustering method and WISE/NEOWISE physical properties. *Astrophys. J.* **770,** 7 (2013).
62. Wetherill, G. W. Steady state populations of Apollo-Amor objects. *Icarus* **37,** 96–112 (1979).
63. Wisdom, J. Chaotic behavior and the origin of the 3/1 Kirkwood gap. *Icarus* **56,** 51–74 (1983).
64. Nesvorný, D. *et al.* Fugitives from the Vesta family. *Icarus* **193,** 85–95 (2008).
65. Russell, C. T. *et al.* Dawn at Vesta: testing the protoplanetary paradigm. *Science* **336,** 684–686 (2012).
66. Thomas, P. C. *et al.* Differentiation of the asteroid Ceres as revealed by its shape. *Nature* **437,** 224–226 (2005).
67. Carry, B. *et al.* Near-infrared mapping and physical properties of the dwarf-planet Ceres. *Astron. Astrophys.* **478,** 235–244 (2008).
68. Castillo-Rogez, J. Ceres—neither a porous nor salty ball. *Icarus* **215,** 599–602 (2011).
69. Gaffey, M. J. *et al.* Mineralogical variations within the S-type asteroid class. *Icarus* **106,** 573–602 (1993).
70. Tholen, D. J. & Barucci, M. A. in *Asteroids II* (eds Binzel, R. P., Gehrels, T. & Matthews, M. S.) 1139–1150 (Univ. Arizona Press, 1989).
71. Lauretta, D. S. *et al.* OSIRIS-REx—exploration of asteroid (101955) 1999 RQ36. *AGU Fall Meet. Abstr.* P21E–01 (2011).
72. Yano, H. *et al.* Hayabusa's follow-on mission for surface and sub-surface sample return from a C-type NEO. In *38th COSPAR Scientific Assembly* 635; http://adsabs.harvard.edu/abs/2010cosp...38..635Y (2010).
73. Barucci, M. A. *et al.* MarcoPolo-R near earth asteroid sample return mission. *Exp. Astron.* **33,** 645–684 (2012).
74. Jenniskens, P. *et al.* The impact and recovery of 2008 TC_3. *Nature* **458,** 485–488 (2009).
75. Brown, P. *et al.* The fall of the Grimsby meteorite—I: Fireball dynamics and orbit from radar, video, and infrasound records. *Meteorit. Planet. Sci.* **46,** 339–363 (2011).
76. Mignard, F. *et al.* The Gaia Mission: expected applications to asteroid science. *Earth Moon Planets* **101,** 97–125 (2007).
77. Jones, R. L. *et al.* Solar System science with LSST. *Earth Moon Planets* **105,** 101–105 (2009).
78. Emery, J. P. & Brown, R. H. Constraints on the surface composition of Trojan asteroids from near-infrared (0.8–4.0 μm) spectroscopy. *Icarus* **164,** 104–121 (2003).
79. Emery, J. P. & Brown, R. H. The surface composition of Trojan asteroids: constraints set by scattering theory. *Icarus* **170,** 131–152 (2004).

80. Emery, J. P., Burr, D. M. & Cruikshank, D. P. Near-infrared spectroscopy of Trojan asteroids: evidence for two compositional groups. *Astron. J.* **141,** 25 (2011).
81. Yang, B. & Jewitt, D. Spectroscopic search for water ice on Jovian Trojan asteroids. *Astron. J.* **134,** 223–228 (2007).
82. Yang, B. & Jewitt, D. A near-infrared search for silicates in Jovian Trojan asteroids. *Astron. J.* **141,** 95 (2011).
83. Fornasier, S. *et al.* Visible spectroscopic and photometric survey of L5 Trojans: investigation of dynamical families. *Icarus* **172,** 221–232 (2004).
84. Fornasier, S. *et al.* Visible spectroscopic and photometric survey of Jupiter Trojans: final results on dynamical families. *Icarus* **190,** 622–642 (2007).
85. Gil-Hutton, R. & Brunini, A. Surface composition of Hilda asteroids from the analysis of the Sloan Digital Sky Survey colors. *Icarus* **193,** 567–571 (2008).
86. Grav, T. *et al.* WISE/NEOWISE observations of the Hilda population: preliminary results. *Astrophys. J.* **744,** 197 (2012).
87. Grav, T., Mainzer, A. K., Bauer, J. M., Masiero, J. R. & Nugent, C. R. WISE/NEOWISE observations of the Jovian Trojan population: taxonomy. *Astrophys. J.* **759,** 49 (2012).

Acknowledgements We are grateful to R. Binzel for help in shaping this review, and to K. Walsh, W. Bottke, N. Moskovitz, D. Polishook, T. Burbine, J. Wisdom and A. Morales for discussions. We thank C. Chapman for a review. We acknowledge support from the ESAC faculty for F.E.D.'s visit. This material is based upon work supported by the National Science Foundation under grant number 0907766 and by the National Aeronautics and Space Administration (NASA) under grant number NNX12AL26G. Any opinions, findings and conclusions or recommendations expressed in this material are those of the authors and do not necessarily reflect the views of the National Science Foundation or NASA. Support for this work was provided by NASA through the Hubble Fellowship grant HST-HF-51319.01-A, awarded by the Space Telescope Science Institute, which is operated by the Association of Universities for Research in Astronomy, Inc., for NASA, under contract NAS 5-26555. F.E.D. is a Hubble Fellow.

Author Contributions Both authors worked jointly on the scientific analysis that resulted in Figs 3 and 4. F.E.D. led the manuscript writing effort and B.C. created the figures.

Author Information Reprints and permissions information is available at www.nature.com/reprints. The authors declare no competing financial interests. Readers are welcome to comment on the online version of the paper. Correspondence and requests for materials should be addressed to F.E.D. (fdemeo@cfa.harvard.edu).